



HAL
open science

Three types of reprojection error on spherical epipolar geometry

Jun Fujiki

► **To cite this version:**

Jun Fujiki. Three types of reprojection error on spherical epipolar geometry. The 8th Workshop on Omnidirectional Vision, Camera Networks and Non-classical Cameras - OMNIVIS, Rahul Swaminathan and Vincenzo Caglioti and Antonis Argyros, Oct 2008, Marseille, France. inria-00325398

HAL Id: inria-00325398

<https://inria.hal.science/inria-00325398>

Submitted on 29 Sep 2008

HAL is a multi-disciplinary open access archive for the deposit and dissemination of scientific research documents, whether they are published or not. The documents may come from teaching and research institutions in France or abroad, or from public or private research centers.

L'archive ouverte pluridisciplinaire **HAL**, est destinée au dépôt et à la diffusion de documents scientifiques de niveau recherche, publiés ou non, émanant des établissements d'enseignement et de recherche français ou étrangers, des laboratoires publics ou privés.

Three types of reprojection error on spherical epipolar geometry

Jun FUJIKI

National Institute of Advanced Industrial Science and Technology,
Umezono, Tsukuba-shi, Ibaraki 305-8568, Japan
jun-fujiki@aist.go.jp

Abstract. To compute an epipolar geometry for spherical images, error evaluation function, which is defined as the sum of squares of reprojection errors, is generally minimized. For pin-hole camera, it is natural to measure the reprojection error as Euclidean distance, which is the quantities defined on image plane. The same as this, for spherical camera, it is natural to measure the reprojection error as the quantities defined on image sphere, not the quantities defined on plane. In this paper, three types of distance are defined as the reprojection error for spherical image. The distances are distance along geodesic, difference of longitude and arc length along colatitude. For three types of distances, the essential matrices for epipolar geometry are computed and the performances are evaluated by comparing to the eight-point algorithm under three-dimensional reconstruction error of synthetic data.

1 Introduction

In computer vision, epipolar geometry for pin-hole camera images[5, 10] is studied as a fundamental and important problem. On the other hand, the computer vision of omnidirectional camera is getting more significant and the epipolar geometry for omnidirectional camera such as large field-of-view camera[3], central-catadioptric[1, 2] and central-dioptric[19] have been investigated. The reason why the omnidirectional cameras are used more and more is that the omnidirectional cameras have wide view of scene compared to pin-hole camera. This means two omnidirectional camera images should have wide common region and many correspondences compare to two pin-hole camera images. Then, the computer vision of the omnidirectional cameras is getting very important.

Among omnidirectional cameras, the camera which has camera center is called central-omnidirectional camera, and the epipolar geometry for central-omnidirectional camera is proposed[7, 17, 19]. There are many kinds of central-omnidirectional cameras are exist, and each kind of central-omnidirectional camera has different way of projection because the central-omnidirectional cameras are constructed with many kinds of mirrors and refractors. Then each kind of central-omnidirectional camera has different kind of image coordinate system. However, all kinds of central-omnidirectional cameras are universally resolved

into spherical camera with spherical perspective projection[19, 7]. Then the analysis of spherical camera is enough to analyse all kinds of central-omnidirectional camera images.

Theoretically, the pin-hole camera is also a kind of the central-omnidirectional camera because the pin-hole camera has camera center. The difference between pin-hole camera and spherical camera is how to fix the freedom of homogeneous image coordinate of image coordinate system. On pin-hole camera, homogeneous image coordinate is fixed by the third component of homogeneous image coordinate is equal to focal length, and on spherical camera, homogeneous image coordinate is fixed by the norm of homogeneous image coordinate is equal to one. Then the pin-hole camera is also resolved into spherical camera, and the analysis of pin-hole camera is instructive for the analysis of spherical camera and vica versa. Especially, the geometrical feature of pin-hole camera represented by homogeneous coordinate is easy to apply to the spherical camera.

In this paper, estimation of epipolar geometry, that is, estimation of essential matrix is highlighted as the useful example of the geometrical feature. Because the epipolar equation for pin-hole camera images is based on the homogeneous coordinate, the epipolar equation for spherical camera has the same representation as the representation of epipolar equation for pin-hole camera[4]. Then any estimation method of essential matrix for calibrated pin-hole camera, including eight-point algorithm[9], can be basically used for calibrated spherical camera.

Although any estimation method for pin-hole camera is applicable to spherical camera, reprojection error, which is the distance between observed data and its estimation, should be measured differently. The reason why reprojection error should be measured differently is that pin-hole camera image is lying on the plane and spherical camera image is lying on the sphere. For the pin-hole camera images, the reprojection error should be measured by the quantities on the plane such as Euclidean distance because the pin-hole camera image is lying on the plane. The same as this, for the spherical camera images, the reprojection error should be measured by the quantities on the sphere because the spherical camera image is lying on the sphere. Then, three types of distances are considered for the spherical camera images in this paper.

For pin-hole camera, algebraic distance, geometric distance and Sampson error is mainly considered. The algebraic distance is the norm of residual vector of the DLT algorithm and this distance is used for eight-point algorithm. The geometric distance is the Euclidean distance between observed and estimated image coordinate on the image plane but it is difficult to treat directly. The Sampson error is an approximation of the geometric distance and this is used for Gold Standard algorithm[10, 13]. The error based on maximum a posterior when the Gauss noise is add to the image coordinate, is also proposed[18]. Note that these problems are unified as the problem of minimizing the distance between observation and estimation under some constraints such as epipolar constraints, like optimal triangulation of image coordinates[12, 14].

For the spherical camera, the most popular reprojection error is a distance along geodesic[11], which is the same as arc length along great circle. In spherical

geometry, geodesic is regarded as line and geodesic is the shortest path between two points on the sphere. Then distance along geodesic for spherical camera image is correspond to the geometric distance for pin-hole camera image. In addition to the distance, two kinds of different distances (reprojection error) are considered in this paper. The one is difference of longitude[6] and another is arc length along colatitude. These two distances are derived from rectification of spherical images. The rectification of spherical image is regarding the epipole as north pole (or south pole) of sphere. By the regarding, the geometrical meaning of epipolar constraint is that corresponding points have the same longitude. From this geometrical feature, two types of reprojection errors based on the rectification are defined. The one is difference of longitude[6] and another is arc length along colatitude. The arc length along colatitude is the weighted difference of longitude of its weights is sine of the colatitude.

In the paper, comparing these three types of reprojection errors through three-dimensional reconstruction computed from the essential matrix. From the experiment by synthetic data, the characteristics of the two types of rectification-based reprojection errors and the distance along geodesic are clarified. Through the paper, least squares criterion is used to define the energy (error) function to compare with eight-point algorithm easily. Of course, there are many works are proposed to derive better estimation than least squares criterion, and it is easy to extend the three types of reprojection errors from least squares criterion to others criterion such as M-estimator criterion, L_∞ -norm criterion etc. However, the least squares criterion is the most appropriate energy function to clarify the difference among reprojection errors because least squares criterion is sensitive to errors and this sensitiveness makes the difference among reprojection errors clear.

As mentioned above, the least squares criterion, which minimizing the sum of squares of distance, is commonly used for error function. But generally, the least squares criterion is easily effected by outliers. Then poor estimation is often obtained from least squares criterion. To overcome the problem, robust estimation against outlier is proposed such as least median of squares (LMedS)[16] or many kinds of M-estimators. but robust estimator sometimes gives local minimum of energy function. Then L_∞ -norm[12] (minimax criterion) estimator, which has no local minimum is also proposed.

2 Epipolar geometry on spherical camera

Calibrated unit spherical camera is used through this paper. In the situation, the spherical camera is the mapping from three-dimensional point \mathbf{X}_p , which is the p -th feature point on spherical camera coordinate system, to two-dimensional unit sphere of its three-dimensional Euclidean coordinate is $\mathbf{z}_p = \frac{1}{\|\mathbf{X}_p\|} \mathbf{X}_p$, which is the p -th feature point on spherical image coordinate system (Fig.1). On spherical camera coordinate system, the points on unit sphere is represented by two parameters which are called colatitude $\phi_p \in [0, \pi]$ and longitude $\psi_p \in (-\pi, \pi]$. The origin of the coordinate system $(\phi_p, \psi_p) = (0, 0)$ is correspond to the

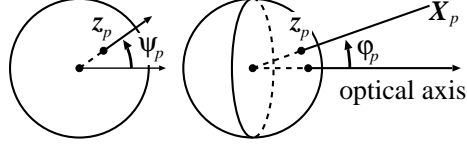


Fig. 1. Spherical camera coordinate system: longitude (left) and colatitude (right) of spherical image z_p

intersection between unit sphere and optical axis. Then the three-dimensional Euclidean coordinate of the origin of spherical camera coordinate system is $\mathcal{N} = (0, 0, 1)^\top$, which is called north pole.

Generally, the three-dimensional Euclidean coordinate of the point on unit sphere z_p is represented by the colatitude ϕ_p and the longitude ψ_p of z_p as

$$z_p = (\sin \phi_p \cos \psi_p, \sin \phi_p \sin \psi_p, \cos \phi_p)^\top. \quad (1)$$

From Eq.(1), the colatitude ϕ_p and the longitude ψ_p of $z_p = (x_p, y_p, z_p)^\top$ is represented as

$$\phi_p = \cos^{-1} z_p, \quad \psi_p = \arg(x_p + iy_p) \quad (2)$$

where i represents imaginary unit.

As already explained, all kinds of central-omnidirectional cameras are universally modeled as the spherical camera[7, 19]. And pin-hole camera is also a kind of central-omnidirectional cameras. Then pin-hole camera is also modeled as the spherical camera. The image coordinate of calibrated pin-hole camera is the gnomonic projection of hemispherical image coordinate (Fig.2). Then, the

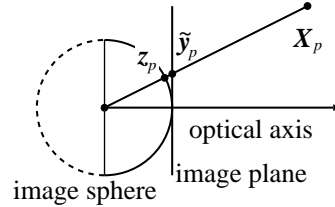


Fig. 2. Spherical image coordinate and pin-hole camera coordinate

mapping from the hemispherical point $z_p = (\sin \phi_p \cos \psi_p, \sin \phi_p \sin \psi_p, \cos \phi_p)^\top$ onto its gnomonic projection $\tilde{y}_p = (\tan \phi_p \cos \psi_p, \tan \phi_p \sin \psi_p)^\top$ is one-to-one mapping from spherical image onto pin-hole camera image.

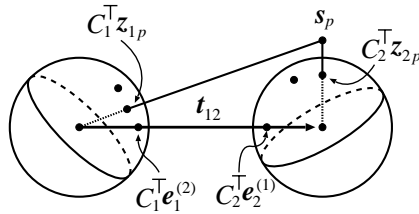


Fig. 3. Epipolar geometry on spherical image

Let $\tilde{\mathbf{y}}_p = (\mathbf{y}_p^\top, 1)^\top$ be a homogeneous coordinate of \mathbf{y}_p , the relation between z_p and \mathbf{y}_p is represented as

$$z_p = \frac{1}{\|\tilde{\mathbf{y}}_p\|} \tilde{\mathbf{y}}_p, \quad \tilde{\mathbf{y}}_p = \frac{1}{(z_p)_3} z_p. \quad (3)$$

where $(z_p)_3$ is the third component of z_p .

Let z_{1p} and z_{2p} be the first and the second spherical image coordinates of the p -th feature points \mathbf{X}_p , respectively. Let \mathbf{y}_{1p} and \mathbf{y}_{2p} be the first and the second pin-hole camera image coordinates corresponding to z_{1p} and z_{2p} as Eq.(3), respectively. Let $\tilde{\mathbf{y}}_{1p}$ and $\tilde{\mathbf{y}}_{2p}$ be homogeneous coordinates of \mathbf{y}_{1p} and \mathbf{y}_{2p} , respectively. And let C_1 and C_2 represent the camera coordinate matrices of the first and the second cameras, which are arraying the basis of the camera coordinate of each camera.

For pin-hole camera, there holds the epipolar equation

$$\tilde{\mathbf{y}}_{1p}^\top E_{12} \tilde{\mathbf{y}}_{2p} = 0 \quad \text{where} \quad E_{12} = C_1 [t_{12}]_\times C_2^\top. \quad (4)$$

The same as the pin-hole camera, there holds the equation

$$z_{1p}^\top E_{12} z_{2p} = 0 \quad \text{where} \quad E_{12} = C_1 [t_{12}]_\times C_2^\top \quad (5)$$

from Eq.(3) (Fig.3). As the same manner as pin-hole camera, E_{12} and Eq.(5) is called essential matrix and epipolar equation for spherical camera, respectively[4]. When a point z_{1p} is selected from the first spherical image, the equation $(z_{1p}^\top E_{12})z = 0$ represents a great circle on the second spherical image. The great circle is called epipolar great circle. Of course, the epipolar great circle is correspond to the epipolar line for pin-hole camera image.

The epipolar great circle pass through the two points on the second spherical image which satisfy $E_{12} \mathbf{e}_2^{(1)} = 0$. These points are called epipoles. One of the epipoles is the image of the first spherical camera center on the second spherical image and another is the antipode of the image of the camera center. As the same manner, the epipoles of the second spherical camera on the first image $\mathbf{e}_1^{(2)\top} E_{12} = 0$ are defined, which are the image of the second spherical camera center on the first spherical image and its antipode.

Note that the representation of these epipoles are

$$\mathbf{e}_1^{(2)} = \pm \frac{1}{\|\mathbf{t}_{12}\|} C_1 \mathbf{t}_{12}, \quad \mathbf{e}_2^{(1)} = \mp \frac{1}{\|\mathbf{t}_{12}\|} C_2 \mathbf{t}_{12}.$$

3 Rectification and spherical epipolar geometry

For pin-hole camera images, the geometrical meaning of rectification is getting the frontal images by changing the optical axis without changing the camera centers. When two pin-hole camera images are obtained, the rectification is the parallelization of two optical axes, and it is realized by projective transformation of pin-hole camera images[10]. After rectification (Fig.4(left)), All epipolar lines are mapped to horizontal lines, and each of the corresponding points lies on the same height.

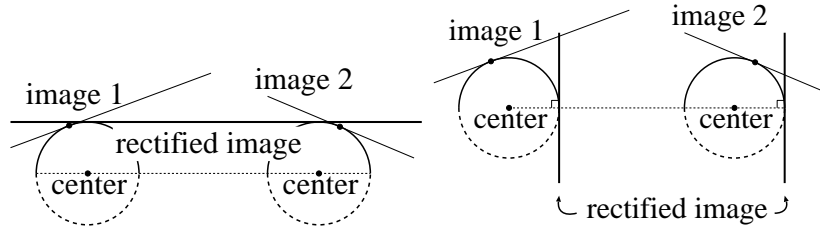


Fig. 4. Rectification of pin-hole camera (left) and spherical camera (right)

For spherical camera image, changing optical axis without changing camera center is equivalent to the rotation of the spherical camera image. Then the rectification of spherical image is realized by rotating spherical image[6]. Of course the rectification of the spherical image can be defined as same as the rectification of the pin-hole camera image as mentioned above, but another rectification can be defined for the spherical image. The concept is very similar to Pollefeys et al.[15], which is the other way of rectification method for pin-hole camera.

The definition of new spherical rectification is rotating the first and the second spherical images to transform epipoles to the north pole $\mathcal{N} = (0, 0, 1)^\top$ or south pole $-\mathcal{N}$. After rectification(Fig.4(right) and Fig.5), All epipolar great circles are mapped to meridian, and each of the corresponding points lies on the same longitude[6].

By the rectification, the representation of epipolar equation become very simple. Let R_1 be a rotation matrix which transforms one of the epipoles of the second spherical camera $\mathbf{e}_1^{(2)}$ to the north pole \mathcal{N} on the first spherical image. And the rotation matrix R_1 also rotate some specific feature point z_{1*} on 0-longitude (longitude pass through Greenwich). Let \mathbf{x}_{1p} be the rectified image (rotated image) of the p -th feature point on the first image z_{1p} , there

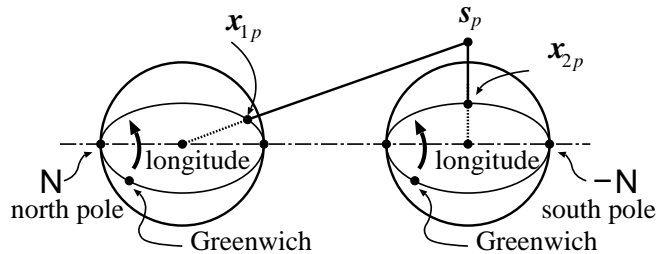


Fig. 5. Epipolar geometry based on longitude

holds $\mathbf{x}_{1p} = R_1 \mathbf{z}_{1p}$. As the same manner, the rotation matrix R_2 , the rectified image of the p -th feature point on the second image $\mathbf{x}_{2p} = R_2 \mathbf{z}_{2p}$ are defined ¹ respectively.

After rectification, the longitudes of \mathbf{x}_{1p} and \mathbf{x}_{2p} should be the same. In this situation, \mathbf{x}_{1p} , \mathbf{x}_{2p} and north pole \mathcal{N} are coplanar (Fig. 5), then there holds

$$\det(\mathbf{x}_{1p} \ \mathbf{x}_{2p} \ \mathcal{N}) = \mathbf{x}_{1p}^\top [\mathcal{N}]_\times \mathbf{x}_{2p} = \mathbf{x}_{1p}^\top \begin{pmatrix} 0 & -1 & 0 \\ 1 & 0 & 0 \\ 0 & 0 & 0 \end{pmatrix} \mathbf{x}_{2p} = 0. \quad (6)$$

This is the epipolar equation after rectification, and the representation of the epipolar equation become very simple.

From Eq.(5) and Eq.(6), the representation of the essential matrix is

$$E_{12} = R_1^\top [\mathcal{N}]_\times R_2. \quad (7)$$

4 Reprojection error

As already explained, the pin-hole camera can be resolved into spherical camera, and the same kind of epipolar equation is hold[4]. This means that any estimation method of essential matrix for calibrated pin-hole camera, including eight-point algorithm[9], can be basically used for calibrated spherical camera. However, the suitable reprojection error, which is the reprojection error is the distance between observed data and its estimation, for spherical camera is different from that for pin-hole camera.

Shortly speaking, the suitable reprojection error for spherical image should be defined by the distance defined on a sphere, as the same as the suitable reprojection error for pin-hole camera should be defined by the distance defined on a plane such as Euclidean distance.

¹ There are two possibilities in computing R_2 when epipole $\mathbf{e}_2^{(1)}$ is transformed to the north pole or south pole. In the two possibilities, the one satisfies the same longitude constraint and another does not satisfy the constraint.

For pin-hole camera, eight-point algorithm is a well-known algorithm. However, the reprojection error for eight-point algorithm is not a geometric distance but an algebraic distance, which is the norm of residual vector of the DLT algorithm. This means the eight-point algorithm is not optimal under the assumption that the image errors are Gaussian. That is, the optimal algorithm should be based on the geometric distance. Because the geometric distance is difficult to treat, the Sampson error is proposed as an approximation of the geometric distance, and the algorithm which minimizes the Sampson error, called Gold Standard algorithm[10, 13] is proposed.

The same as this, For the spherical camera images, the reprojection error should be measured by the quantities on the sphere. Then, three types of distances are considered for the spherical camera images. The first one is the distance along geodesic[11], which is the most popular reprojection error on the sphere. The distance along geodesic is the same as arc length along great circle. In spherical geometry, geodesic is regarded as line because geodesic is the shortest path between two points on the sphere. Then distance along geodesic for spherical camera image is correspond to the geometric distance for pin-hole camera image.

In addition to the distance along geodesic, two kinds of different distances (reprojection error) are considered in this paper. The one is difference of longitude[6] and another is arc length along colatitude. These two distances are derived from rectification of spherical images. As explained in previous section, the corresponding points in two sperical images are lying on the same longitude after rectification. Then it is natural to measure the distance between two corresponding points by the difference of longitude. However, when some point is lying near the north or south pole of the sphere, small noise on the point makes large difference of longitude. To deduce this, adding small weight to the point near the north or south pole of the sphere. When the weight is computed as the sine of the colatitude, the weighted difference of longitude is equivalent to the arc length along colatitude. Therefore, these three types of reprojection error, which are defined by the quantities on the sphere, is used in this paper.

Let e be the epipole and z_p be the some feature point on the spherical image. And let R be a rotation matrix which transforms epipole e to north pole \mathcal{N} and specific image coordinate z_* onto 0-longitude meridian. In this situation, the relationship between the point z_p on the spherical image and the point x_p on the rectified image is represented as $x_p = Rz_p$.

Let ϕ_p and ψ_p be the colatitude and the longitude of x_p which is a point on the one image, respectively. And let α_p be a longitude of meridian (epipolar great circle) on another image corresponding to x_p .

In this situation, the three types of “error”s of each datum are defined as follows:

- Distance along geodesic: $Err_p = \sin^{-1}\{\sin \phi_p \sin(\psi_p - \alpha_p)\}$.
- Difference of longitude: $Err_p = \psi_p - \alpha_p$.
- Arc length along colatitude: $Err_p = \sin \phi_p(\psi_p - \alpha_p)$.

The distance along geodesic is computed by the spherical trigonometry for right spherical triangle.

For each “error”s, error function is defined as $J = \frac{1}{2} \sum_p Err_p^2$, and the error function J is minimized by changing Euler angles² of two rotation matrix R_1 and R_2 defined in previous section (6 parameters) under Levenburg-Marquardt algorithm provided by Optimization Toolbox on MATLAB.

Let R^{new} be the updated quantity of the rotation matrix computed by LM algorithm, the representation of the updated epipole and points on the spherical image are

$$\mathbf{e}^{\text{new}} = (R^{\text{new}})^\top \mathcal{N}, \quad \mathbf{x}_p^{\text{new}} = R^{\text{new}} \mathbf{z}_p. \quad (8)$$

5 Algorithms

5.1 Initial estimation

- (1) Estimate the essential matrix E_{12} by eight-point algorithm.
- (2) Compute the epipoles $\pm \mathbf{e}_1^{(2)}$ and $\pm \mathbf{e}_2^{(1)}$.
- (3) Compute the rotation matrix R_1 .
- (4) Compute the rotation matrix $R_2^{\mathcal{N}}$ or $R_2^{-\mathcal{N}}$ or which transforms $\mathbf{e}_2^{(1)}$ to north pole \mathcal{N} or south pole $-\mathcal{N}$, respectively, and compute energy function J for both matrix to select the pair of R_2 and $\mathbf{e}_2^{(1)}$ which minimize the energy function J .

5.2 Estimation of epipoles based on rectification

- (1) Compute $\mathbf{x}_{ip} = R_i \mathbf{z}_{ip}$ ($i = 1, 2$) from initial estimation.
- (2) Compute infinitesimal rotation matrix which decrease J for R_1 and R_2 simultaneously by LM algorithm.
 - (a) Compute the longitude α_{1p} of \mathbf{x}_{1p} , and compute the colatitude ϕ_{2p} and longitude ψ_{2p} of \mathbf{x}_{2p} . And compute energy function J_2 . And compute the longitude α_{2p} of \mathbf{x}_{2p} , and compute the colatitude ϕ_{1p} and longitude ψ_{1p} of \mathbf{x}_{1p} . And compute energy function J_1 . And make a sum of J_1 and J_2 . ($\alpha_{ip} = \psi_{ip}$).
 - (b) Compute R^{new} by LM algorithm, and update the epipoles \mathbf{e}_i , and rectified spherical image \mathbf{x}_{ip} .
- (3) After convergence, the estimations of the rotation matrix R_1 and R_2 are obtained, and the estimation of the essential matrix is $E_{12} = R_1^\top [\mathcal{N}]_\times R_2$.

² When parameter manifold is not flat, tangent vector of the manifold is generally going outside of the manifold. Then by using tangent vector on rotation matrix manifold to update estimation, updated value is no longer rotation matrix. So, the updated value should be projected to the rotation matrix manifold. To avoid this, the Euler angle representation of rotation matrix is used to compute rotation matrix in the paper. Other method to avoid this, Riemannian Newton's Algorithm[14], which is the Newton's method on manifold by using exponential map, is proposed. Note that the exponential map of the rotation matrix is represented by Rodrigues' formula of rotation matrix. Then the steepest gradient method by using Rodrigues's formula of rotation matrix[6] is the minimization problem on Riemannian space.

6 Numerical experiments by synthetic data

To clarify the characteristics of the three types of reprojection errors, the numerical experiment by synthetic data is investigated ³.

The three-dimensional feature points and its spherical images for numerical experiments are generated as follows:

- The three-dimensional feature points are randomly selected by uniform distribution on three-dimensional cube whose center of gravity is at the origin of the world coordinate system.
- The points in three-dimensional space are projected onto points z_{1p} and z_{2p} on the spherical images of the cameras of camera centers are c_1 and c_2 , respectively.
- Add noise from uniform distribution of a disk of center z_p and radius ϵ for each point z_{1p} and z_{2p} . The ϵ is called noise variance in the paper.

The reconstruction error is evaluated by the sum of square distance between the estimated three-dimensional points and the corresponding points of the ground truth. Generally, the three-dimensional reconstruction of the object has 7 degree of freedom (DOF). Therefore, these degree of freedom should be fixed to compare the estimation with the ground truth. Among the 7 DOF, 3 DOFs is for translation, 3 DOFs is for rotation and the rest 1 DOF is for global scale parameter. By giving the camera center of the ground truth, 3 DOFs for translation, 2 DOFs is for rotation and 1 DOF is for global scale parameter can be fixed and the only 1 DOF is remaind. The rest 1 DOF is rotation around the line connecting two camera centers. The rest 1 DOF is fixed by estimating the rotation to minimize the sum of square distance between the estimated three-dimensional points and corresponding points of the ground truth. Then, all 7 DOFs are fixed. After 7 DOFs are fixed, the reconstruction error is computed by the sum of square distance between the estimated three-dimensional points and the corresponding points of the ground truth.

This procedure is repeated T times, and results are statistically evaluated. The error of three-dimensional reconstruction is measured by median of T times trial. Through the experiments, the ground truth of two rotation matrix R_1 and R_2 is identity matrix I , and the three-dimensional Euclidean coordinate of two camera center is $c_1 = (4, 0, 0)^T$ and $c_2 = (-4, 0, 0)^T$, the edge of the data-generateing cube is 40, and the trial times is $T = 1000$.

6.1 Evaluation w.r.t. changes of numbers of correspondences

Figure 6 shows the results of the numerical experiments in which the number of three-dimensional points P is increased from 20 to 200 with the interval 10. The noise variance of a point on a spherical image is fixed to $\epsilon = 0.01$. In Fig.6, the horizontal axis is the number of points and the vertical axis is the median of the

³ The program by MATLAB is provided at

<http://cmp.felk.cvut.cz/~torii/public/release/s2lopt.zip>

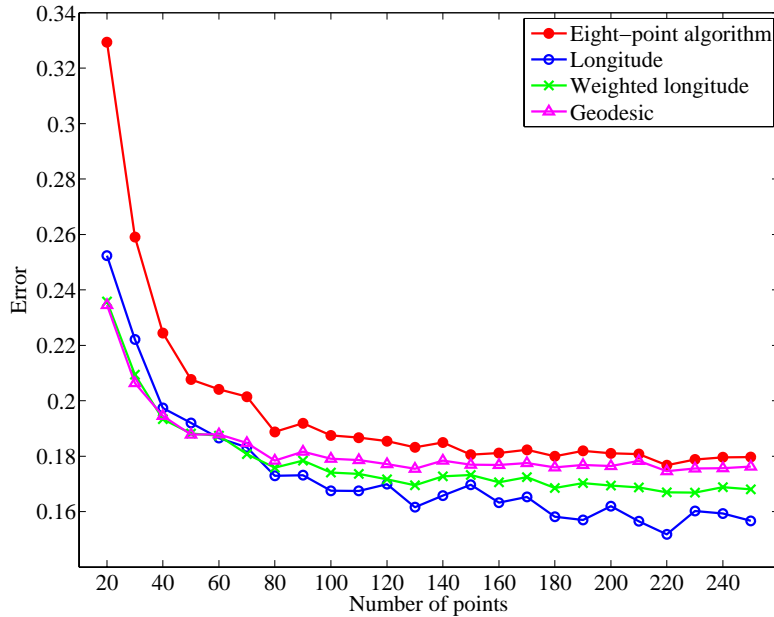


Fig. 6. Evaluation w.r.t. changes of numbers of correspondences

three-dimensional reconstruction error. The error by the eight-point algorithm and the rectification-based methods are plotted as follows:

- Eight-point algorithm: Red lines and bullet “•”.
- Difference of longitude: Blue lines and circular “o”.
- Arc length along colatitude: Green lines and cross “×”.
- Distance along geodesic: Magenta lines and triangle “△”.

From the experiments, all of rectification-based methods show positive results compare to the eight-point algorithm. When the number of corresponding points are less, distance along geodesic and arc length along colatitude is better to measure the distance from the image points to epipolar great circle. And when the number of corresponding points are many, difference of longitude is better to measure the distance from the image points to epipolar great circle.

6.2 Evaluation w.r.t. changes of noise variance

Figure 7 shows the results of the numerical experiments in which the noise variance ϵ is increased from 0.2 to 2.0 with the interval 0.2. The number of corresponding points is fixed to $P = 100$. In Fig.7, the horizontal axis is the noise variance and the vertical axis is the median of the three-dimensional reconstruction error. The error by the eight-point algorithm and the rectification-based methods are plotted as same manner as previous experiment.

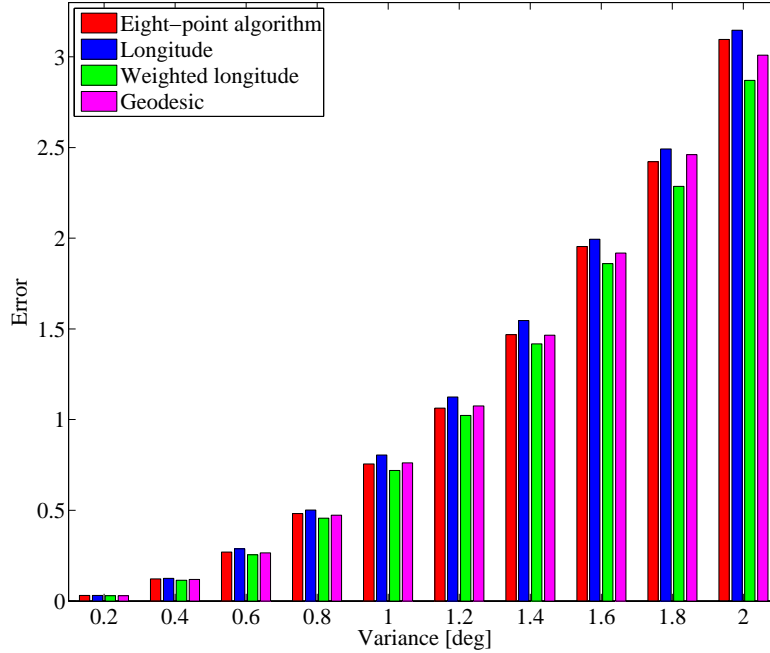


Fig. 7. Evaluation w.r.t. changes of noise variance

From the experiments, arc length along colatitude gives positive result compare to the eight-point algorithm, distance along geodesic gives not negative result compare to the eight-point algorithm and difference of longitude gives negative result compare to the eight-point algorithm. This tendency is notable when the error variance is large. When the error variance is small, all method makes little difference, but when the error variance is large, arc length along colatitude is the most appropriate distance to measure the error.

6.3 View of three-dimensional reconstruction

Figure 8 shows the three-dimensional reconstruction of a cube for the reference. The data of the ground truth is plotted with black lines and square “□”. The rest of data are plotted as the same manner as previous experiments. The result of experiment shows the rectification-based methods derives better reconstruction than eight-point algorithm.

7 Conclusion and discussion

In the spherical camera model, the rectification is the transforming the epipole of each image to the north and/or south pole by rotation. In the sense, the mean-

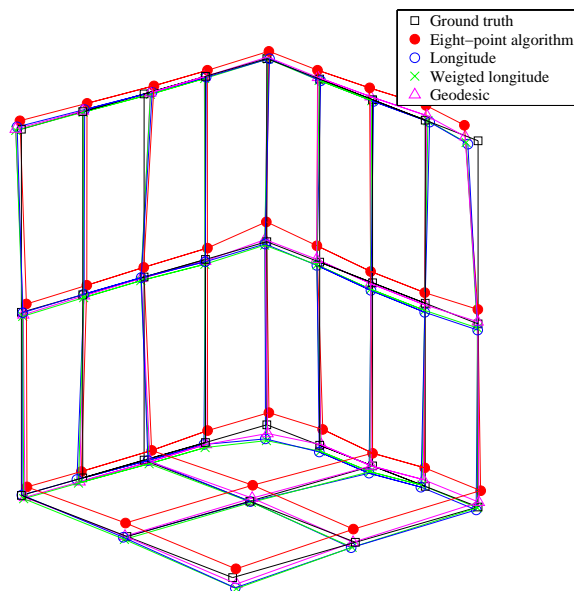


Fig. 8. three-dimensional reconstruction of cube

ings of epipolar constraint is the corresponding points should lie on the same longitude, and two types of reprojection error can be defined as the difference of longitude and the arc length along colatitude.

In the paper, these two types of reprojection error and the distance along geodesic are compared with eight-point algorithm. From the experiment by synthetic data, the characteristics of the two types of rectification-based reprojection error and the distance along geodesic are clarified. The mathematical and/or geometrical meanings of the result is not clear, but some qualitative discussion can be done. When noisy data are distributed around epipole, difference of longitude is not suitable to measure errors. However, the number of data is increasing, the rate of data around epipole is decreasing. Then difference of longitude is suitable to measure errors. To estimate epipolar geometry robustly, the arc length along colatitude is suitable to measure errors. When errors are measured by the difference of longitude and/or the arc length along colatitude, the epipole may be well estimated because the errors are computed based on the longitude. This means the estimation based on these errors are appropriate for robust estimation of epipole. This robustness may be closely related to the behavior of experiments for longitude based error.

8 Acknowledgements

The author would like to thank Dr. Akihiko Torii, Researcher of Center for Machine Perception of Czech Technical University, for supporting the experiment and helpful discussions.

References

1. S. Baker and S. K. Nayar. A theory of single-viewpoint catadioptric image formation. *International Journal of Computer Vision*, vol. 35(2), pp. 175–196, 1999.
2. J. P. Barreto and K. Daniilidis. Unifying image plane liftings for central catadioptric and dioptric cameras. In *OMNIVIS '04*, pp. 151–162, 2004.
3. R. Benosman and S. B. Kang, editors. *Panoramic Vision: Sensors, Theory, Applications*. Springer-Verlag, 2001.
4. P. Chang and M. Hebert, Omni-directional structure from motion, In *OMNIVIS '00*, pp. 127–133, 2000.
5. O. Faugeras, Q. T. Luong, and T. Papadopoulou. *The Geometry of Multiple Images: The Laws That Govern The Formation of Images of A Scene and Some of Their Applications*. MIT Press, Cambridge, MA, USA, 2001.
6. J. Fujiki, A. Torii and S. Akaho, Epipolar Geometry via Rectification of Spherical Images, In *MIRAGE '07*, pp. 461–471, 2007.
7. C. Geyer and K. Daniilidis, Catadioptric projective geometry. *International Journal of Computer Vision*, vol. 45(3), pp. 223–243, 2001.
8. C. Geyer and K. Daniilidis, Properties of the catadioptric fundamental matrix, *ECCV '02*, vol. 2, pp. 140–154, 2002.
9. R. I. Hartley, In defence of the eight-point algorithm, *IEEE Trans. PAMI*, vol. 19, no. 6, pp. 580–593, 1997.
10. R. Hartley and A. Zisserman, *Multiple view geometry in computer vision*, Cambridge University, Cambridge, 2nd edition, 2003.
11. R. I. Hartley and F. Kahl, Global optimization through searching rotation space and optimal estimation of the essential matrix, *ICCV '07*, 2007.
12. F. Kahl, Multiple view geometry and the L_∞ -norm, *ICCV '05*, pp. 1002–1009, 2005.
13. Y. Kanazawa and K. Kanatani, Reliability of 3-D reconstruction by stereo vision, *IEICE Trans. Inf. & Syst.*, vol. E78-D-10, pp. 1301–1306, 1995.
14. Y. Ma, J. Kosecka and S. Sasty, Optimization criteria and geometric algorithms for motion and structure estimation, *IJCV*, vol. 44(3), pp. 219–249, 2001.
15. M. Pollefeys, R. Koch and L. V. Gool, A simple and efficient rectification method for general motion, *ICCV '99*, pp. 496–501, 1999.
16. R.J.Rousseeuw and A.M.Leroy, *Robust Regression and Outlier Detection*, John Wiley & Sons, NY, 1987.
17. T. Svoboda and T. Pajdla, Epipolar Geometry for Central Catadioptric Cameras. *IJCV*, vol. 49(1), pp. 23–37, 2002.
18. J. Weng, T. S. Huang and N. Ahuja, Optimal motion and structure estimation. *PAMI*, vol. 15(9), pp.864–884, 1993.
19. X. Ying and Z. Hu. Can we consider central catadioptric cameras and fisheye cameras within a unified imaging model. In *ECCV '04*, vol. 1, pp. 442–455, 2004.